COMMUNICATIONS IN COMPUTATIONAL PHYSICS
Vol. **3**, No. 5, pp. 1051-1070

Commun. Comput. Phys.
May 2008

The Role of Anionic Protein Residues on the Salt Dependence of the Binding of Aminoacyl-tRNA Synthetases to tRNA: A Poisson-Boltzmann Analysis

Johan H. Bredenberg[1], Alexander H. Boschitsch[2] and Marcia O. Fenley[1,3,*]

[1] *Institute of Molecular Biophysics, Florida State University, Tallahassee, FL 32306, USA.*
[2] *Continuum-Dynamics Inc., 34 Lexington Avenue, Ewing, NJ 08618, USA.*
[3] *Department of Physics, Florida State University, Tallahassee, FL 32306, USA.*

Received 26 October 2007; Accepted (in revised version) 18 December 2007

Available online 25 January 2008

Abstract. Long-range electrostatic interactions in proteins/peptides associating to nucleic acids are reflected in the salt-dependence of the binding process. According to the oligocationic binding model, which is based on counterion condensation theory, only the cationic residues of peptides/proteins near the binding interface are assumed to affect the salt dependence in the association of peptides and proteins to nucleic acids. This model has been used to interpret and predict the binding of oligocationic chains - such as oligoarginines/lysines - to nucleic acids, and does an excellent job in these kinds of systems. This simple relationship, which is used to compare or count the number of ionic interactions in protein-nucleic acid complexes, does not hold when acidic residues, *i.e.* glutamate and aspartate, are incorporated in the protein matrix. Here, we report a combined molecular mechanics (by means of energy-minimization of the structure under the influence of an empirical energy function) and Poisson-Boltzmann (PB) study on the salt-dependence in binding to tRNA of two important enzymes that are involved in the seminal step of peptide formation in the ribosome: Glutamine synthetase (GluRS) and Glutaminyl synthetase (GlnRS) bound to their cognate tRNA. These two proteins are anionic and contain a significant number of acidic residues distributed over the entire protein. Some of these residues are located in the binding interface to tRNA. We computed the salt-dependence in association, SK_{pred}, of these enzyme-tRNA complexes using both the linear and nonlinear solution to the Poisson-Boltzmann Equation (PBE). Our findings demonstrate that the SK_{pred} obtained with the nonlinear PBE is in good agreement with the experimental SK_{obs}, while use of the linear PBE resulted in the SK_{pred} being anomalous. We conclude that electrostatic interactions between the binding partners in these systems are less favorable by means of charge-charge repulsion between negatively charged protein residues and phosphate-oxygens in the tRNA backbone but also play a significant role in the association process

*Corresponding author. *Email addresses:* jbreden@sb.fsu.edu (J. H. Bredenberg), alex@continuum-dynamics.com (A. H. Boschitsch), mfenley@sb.fsu.edu (M. O. Fenley)

of proteins to tRNA. Some unfavorable electrostatic interactions are probably compensated by hydrogen-bonds between the carboxylate group of the side chain in the interfacial acidic protein residues and the tRNA backbone. We propose that the low experimentally observed SK_{obs} values for both GlnRS- and GluRS-tRNA depend on the distribution and number of anionic residues that exist in these tRNA synthetases. Our computed electrostatic binding free energies were large and unfavorable due to the Coulombic and de-solvation contribution for the GlnRS-tRNA and GluRS-tRNA complexes, respectively. Thus, low SK_{obs} values may not reflect small contributions from the electrostatic contribution in complex-formation, as is often suggested in the literature. When charges are "turned off" in a computer-experiment, our results indicated that "turning off" acidic residues far from a phosphate group significantly influences SK_{pred}. If cationic residues are "turned off", less impact on SK_{pred} is observed with respect to the distance to the nearest phosphate-group.

AMS subject classifications: 35Q80, 92C05, 92C40, 65N06

Key words: Enzyme, electrostatics, molecular mechanics, Poisson-Boltzmann equation, oligocation, salt-dependence, aminoacyl-tRNA synthetase, polyelectrolyte, counterion condensation theory.

---

1 Introduction

The association of aminoacyl-tRNA synthetase (aaRS) to transfer RNA (tRNA) is important in various biological events such as the protein biosynthetic machinery, signal transduction and regulation mechanisms [1–3]. Aminoacyl-tRNA synthetases, which are an important class of information-processing enzymes, are highly negatively charged at physiological conditions yet bind to a highly negatively charged partner: tRNA. At first, since both tRNA and aaRS are negatively charged biomolecules and repel each other according to the basic laws of physics, one would not expect that they can form a stable complex. However, some studies suggest that the positive surface potential and the field extending from it, which is created by the cationic enzyme residues, help drive the attraction between the tRNA and aaRS at long distances (*e.g.*, [4]). Different studies have indeed shown that the electrostatic interactions are very important in various aspects of the biological function of this class of tRNA-enzyme complexes [5–7]. For instance, the specificity and strength of the interaction between different natural/cognate substrates/analogs and aminoacyl-tRNA synthetase enzymes can be optimized (in the computer and later on in the lab by site-directed mutagenesis) by changing the charge distribution and thereby adjusting the short-range (hydrogen-bonds and salt bridges) and long-range electrostatic interactions [5–7].

Banerjee and co-workers report tryptophan fluorescence quenching experiments that resulted in a rather low SK_{obs} for the salt dependence in the association of both GluRS and GlnRS to tRNA [8]. The authors rule out that any coupled folding-unfolding events

of both binding partners were responsible for these low values of SK_{obs}, since some studies [8, 9] indicated that the changes in the tRNA and aaRS structures upon binding were small. They also proposed that the low component of the electrostatic contribution to the total binding energy and low ion release stoichiometry was due to the more electroneutral nature of the protein interaction domain, due to the presence of a significant number of negatively charged protein residues near the binding interface. Here, we followed up on these observations and examined more closely the role of the anionic residues that are both close and far from the sugar-phosphate backbone, upon the salt dependence of the binding process of aaRS to tRNA.

Given that the binding interface for the GluRSs and GlnRSs are quite large (> 2200 Å^2) and many cationic residues are in close proximity to the phosphate backbone, the authors of this study found less correlation between the slope of the linear log-log plot of the binding constant (K_{obs}) versus salt concentration (commonly referred to as SK_{obs} in the literature) and the number of cationic protein residue-phosphate contacts. According to the Record-Lohman oligocation model [10], which is based on the well-founded counterion condensation theory developed by Jerry Manning [11], the absolute value of SK_{obs} should be directly proportional to the number of "ionic contacts" (*i.e.*, salt bridges between cationic peptide or protein residues and nucleic acid phosphates) at the binding interface. Any prediction of SK_{obs} is thus from hereon called SK_{pred}. It seems that the oligocation binding model does not hold for the GlnRS and GluRS complexes examined in this study. A similar trend was also observed for other protein-DNA complexes, such as the integration host factor protein, TF1 (a bacterial histone-like HU homologue) and the halophilic TATA-box binding protein (TBP) binding to DNA [12–14]. The Record group suggests that the larger values of SK_{pred} (obtained from the number of ion pairs deduced from the X-ray structure of the complex and applying Eq. (2.3) below) compared with the actually observed experimental SK_{obs} for DNA binding proteins that wrap around DNA, are due to the disruption of surface salt bridges that are coupled to DNA binding [15].

Interestingly, there are some common features between the aaRS-tRNA complexes, IHF-DNA [15] complexes and thermophilic/halophilic TBP-DNA [13] complexes. First, the binding interfaces are quite extensive and polar and a substantial number of ionic contacts are made between phosphate groups and cationic protein residues. Surprisingly, however, there is also a large number of anionic residues quite near the binding interface. This result is consistent with structural analysis of various RNA-protein complexes where the interface seems to have some anionic protein residues, although the propensity is in fact very low compared to cationic residues such as Lys and Arg [16]. Actually, in one such structural analysis where 1/3 of the dataset of RNA-protein complexes was composed of tRNA-aaRS complexes it was found that the propensity of having Glu and Asp residues in the binding interface of nucleic acid-protein complexes is larger for RNA-protein complexes relative to DNA-protein complexes [17]. Thus, we propose that the anionic residues can have a large impact on the salt dependence of binding as opposed to the common view that only cationic residues near the binding interface are controlling

the SK_{obs}. Actually, the fact that anionic peptide and protein side chains play a role in the salt dependence of the binding process has been observed in some recent thermodynamic binding studies of protein/peptide-nucleic acid complexes reported in the literature [13–15, 18].

Our main goal in this paper is to examine the salt dependence of the binding of GluRS and GlnRS to tRNA using both the linear and nonlinear Poisson-Boltzmann Equation (PBE) in order to verify how these PBE predictions compare against experimental results [8]. The motivation for this first goal stems from the fact that some recent computational studies have been examining different aspects of the specificity and strength of binding interactions in highly charged tRNA-aaRS complexes [5, 7] using the more approximate linear Poisson-Boltzmann equation as opposed to the nonlinear PBE. Some limitations of linear PBE predictions for this highly charged nucleic acid-enzyme system have been pointed out previously in the literature [5, 7]. Our second goal is to examine how well the oligocation binding model applies to the GluRS- and GlnRS-tRNA systems. The third goal is to explain why SK_{obs} are low based on our nonlinear PBE approach and analysis of the charge distribution of these class I tRNA synthetases. Our last goal is to verify whether the contribution of the electrostatic interactions to the binding reaction between tRNA and aaRS is in fact small as suggested in the literature [8].

Our Poisson-Boltzmann analysis of the aaRS-tRNA binding process leads us to the following conclusions: 1) The linear PBE can overestimate the magnitude of SK_{pred} by orders of magnitude and predict the incorrect sign when compared against SK_{obs} from experimental thermodynamic data; 2) SK_{pred} based on nonlinear Poisson Boltzmann agrees well with the experimental SK_{obs} and 3) the low values of the magnitude of SK_{obs} can be explained by the large number of charge-charge repulsions that are largely dominant in the interaction between the anionic aaRS and tRNA. These charge-charge repulsions result in unfavorable Coulomb energies when the aaRS has a larger negative overall charge, but appear to be compensated by hydrogen bonds between the aaRS acidic side chains and backbone of the nucleic acid chain and are screened by solvent molecules 4) the oligocationic binding model does not apply in this protein-RNA system since the slope is dictated by the overall charge distribution of the aaRS and not only the cationic or anionic residues at or near the binding interface.

2 Methods and theory

2.1 Preparation of the aaRS-tRNA structures

We selected two aaRS-tRNA complex structures that have experimental salt-dependent binding thermodynamic data reported in the literature [8]. The following 3D structures were retrieved from the Protein Data Bank (PDB) (`http://www.rcsb.org/pdb`) and used in this work: Glutamyl-tRNA synthetases (pdb codes: 1G59 [9] and 1N77 [19], Glutaminyl-tRNA-synthetases (pdb codes: 1O0B [20] and 1QTQ [21]). The main analysis concerns X-ray structures 1G59 (GluRS) and 1QTQ (GlnRS) since they are higher in

resolution. The other two structures served as controls in our Poisson-Boltzmann equation (PBE) calculations.

All structures were optimized with the CHARMM [22] program and the CHARMM all-atom 22/27 [23,24] force field parameters and topology files for proteins and nucleic acids. Any co-existing crystal oxygen water atoms, ions, substrates or other prosthetic groups not defined as enzymes associated to tRNA were removed and were not included in our calculations. Missing atoms and/or residues were constructed from the internal coordinates as defined in the CHARMM22/27 residue topology files for protein and nucleic acids, respectively, and hydrogen atoms were positioned with HBUILD [25]. All non-bonded electrostatic interaction energies and forces between atom pairs were set to the default values as described in the CHARMM22/27 parameter files [23, 24]. The Coulomb energy was smoothly truncated to zero at 12 Å, using an atom-based spherical shifting function, and the vdW (*i.e.* Lennard-Jones 6, 12 interactions) were treated with an atom-based switching function at 12 Å [26]. The non-bonded listing involved atoms within 14 Å distance from each other. This list was regenerated whenever an atom had moved 1 Å since the last update. Keeping all non-hydrogen atoms frozen, 200 steps of Steepest Descent (SD) followed by 500 steps of Adopted Basis Newton Raphson (ABNR) minimization were carried out. All atoms were then released and a mass-weighted harmonic force constant of 25 kcal mol^{-1} Å^{-2} was applied on all non-hydrogen atoms. A second round of 200 steps of SD and 1,000 steps of ABNR minimization was executed and the resulting minimized coordinates were then used in the computational protocol for solving the Poisson-Boltzmann equation.

2.2 Structure analysis

We defined a charge-charge pair based on the minimum distance between the Asp-, Glu-carboxylate oxygen or Arg-, Lys-amide nitrogen atoms on the protein side-chain to the nucleic acid phosphate-oxygen atoms, and thus each charge-pair is only counted once within a certain threshold for the boundary (here taken as pairs within the region of zero to four Å and within the region of four to six Å as suggested in the literature [27]). A hydrogen bond is considered present whenever the distance from the hydrogen to the acceptor atom is ≤ 2.4 Å as set in the CHARMM program (see hbonds.doc in the documentation for CHARMM). For solvent-mediated bridges between the aaRS and tRNA, we included any heavy atom that mutually was ≤ 3.0 Å from any of the aaRS and tRNA atoms. While the choice of distances for deciding which atoms that are forming solvent-mediated is somewhat arbitrary, visual inspection of the structures justified the choice of 3.0 Å to be reasonable.

2.3 Poisson-Boltzmann calculations

The 3D PBE approach is now widely used to model salt-mediated electrostatic screening effects in biomolecular applications and many different numerical methods have been

employed in order to solve this nontrivial and numerically challenging second order partial differential equation, especially its nonlinear form (*e.g.*, [28, 29]). The current study employed a finite difference method to solve the PBE implemented on an adaptive mesh whose resolution is finest at the molecular surface and coarser elsewhere. Inside the molecule, the PBE solver calculates the reaction field potential thus eliminating singularities at the charge sites [28]. In the exterior region the usual potential field was solved for. These features allow accurate PBE predictions to be obtained without the need for focusing techniques [30]. The PBE solver also contains a robust multi-grid procedure that reliably and efficiently converge the highly nonlinear PB solution, which is vital for modeling highly charged biomolecular systems. Finally, an outer boundary treatment derived from charge conservation principles was used to set the outer boundary potential for both linear and nonlinear calculations and enforce neutrality [31]. For the results presented here the finest mesh spacing at the surface was 0.3 Å. Electrostatic binding free energies were computed from three separate PB calculations: one for each of the two molecules considered in isolation and a third for the complex. To minimize grid sensitivity, all three calculations were conducted on the same mesh.

All linear or nonlinear finite-difference based PBE calculations were set at neutral pH (7.0) and room temperature (298 K). We varied the 1:1 salt (NaCl) concentration from 0.1 to 0.4 M since the linearity of the electrostatic binding free energy as a function of the logarithmic of 1:1 salt holds in this range. The solute (here the protein, tRNA or complex) was treated as a low dielectric region ($\varepsilon_{\text{in}} = 2$) immersed in a high dielectric region ($\varepsilon_{\text{out}} = 80$). The use of $\varepsilon_{\text{in}} = 2$ is justified since the salt-derivative electrostatic binding free energy is fairly independent of the choice of the interior dielectric constant (results not shown). Here we have not addressed how the presence of $MgCl_2$ in the buffer affects SK_{pred} but will address this important issue in another communication. The solvent excluded molecular surface, which was based on a water probe radius of 1.4 Å, was used to define the dielectric interface that separates the solute and solvent regions. No ion exclusion region was considered but the salt derivative of the electrostatic binding free energies is not very sensitive to its presence (results not shown). The charges and the atomic radii, which we used to define the dielectric interface for the different atom types, were taken from the CHARMM22/27 parameters [23, 24] with one exception: The radii of hydrogen atoms bound to atoms that are donor- or acceptor-atoms (*e.g.*, oxygen or amide-nitrogen atoms) were set to 1 Å, since the original radii of 0.2245 Å for donor-acceptor type hydrogen atoms is small compared to the mesh size and may result in small numerical errors for the NLPB calculation. However, this setting of the hydrogen radii does not change the conclusions in this work. We model a physiological pH of 7.0 by assuming the charged protein residues in their ionized forms for Asp, Glu, Arg, Lys and the amino and carboxyl termini. It will be important to consider the possibility that certain histidines can become protonated upon binding to tRNA [32]. It is also possible that some anionic enzyme residues that lie close to the sugar-phosphate backbone (surrounded by a clustering of negatively charged groups) could have altered protonation states upon binding to tRNA, as suggested by an experimental study that examines

the role of active site carboxylate residues on the binding specificity of *Mun*I restriction endonuclease to DNA [33]. Thus, a careful study of protonation states of His, Asp and Glu will be important in order to correctly predict the SK_{obs} values. However, our main goal is not to reproduce the experimental values of SK_{obs}, which in principle can only be correctly predicted if at least the protonation states and conformational adaptability are properly modeled.

2.4 Visualization of the electrostatic potential on the molecular surface

The molecular surfaces were color coded according to electrostatic potential derived from the non-linear PBE and were rendered using the Virtual Reality Modeling Language (VRML) developed by the NIST (`http://www.nist.gov/`). The coarse representation of the tRNA structure was displayed with the PYMOL program (`http://pymol.sourceforge.net`) and then incorporated into the electrostatic potential maps for easy identification. In order to facilitate visual inspection, color mapping of the electrostatic potential was finely scaled as follows: green (most positive), followed by blue, white (neutral), red and yellow (most negative).

2.5 Salt dependence of the electrostatic binding free energy

In some biomolecular processes, such as the binding of a charged ligand to nucleic acids, it is usually appropriate to assume that the salt dependence of the total binding free energy is solely determined by the long-range electrostatic interactions. Based on this assumption one can make a connection between the experimental thermodynamic results, SK_{obs}, and computed PB-results, SK_{pred}, from the following relationship [10]:

$$SK_{obs} = \frac{d\log K_{obs}}{d\log[M^+]} = -\frac{d\Delta G_{elec}}{2.3kTd\log[M^+]} = SK_{pred}, \tag{2.1}$$

where ΔG_{elec} is the electrostatic binding free energy (in units of kT), k is the Boltzmann constant, T is the absolute temperature (here taken as 298K), $[M^+]$ is the 1:1 salt concentration (here NaCl) and K_{obs} is the observed binding constant. The electrostatic binding free energy was computed by taking the difference between the electrostatic binding free energy of the complex and the electrostatic free energy of the individual binding partners in their docked state (*i.e.*, in its bound state as opposed to its unbound state) at a fixed 1:1 salt concentration. The calculation of ΔG_{elec} involves three separate PBE calculations of G_{elec}: one for the protein-tRNA complex, one for the isolated tRNA and one for the isolated protein. Thus, the electrostatic binding free energy, ΔG_{elec}, is expressed as

$$\Delta G_{elec} = G_{elec}(\text{complex}) - G_{elec}(\text{protein}) - G_{elec}(\text{tRNA}), \tag{2.2}$$

where the first term on the right-hand side of Eq. (2.2) is the electrostatic free energy of the complex and the two other terms represent the electrostatic free energy of the protein

and tRNA, respectively. It is important to stress that correctly modeled protonation effects are needed in the estimate of SK_{pred}. All we are computing is SK_{pred} based on the rigid docking (*i.e.*, lock-in-key) reaction, where we assumed that the conformational state of the binding partners were the same in the bound and unbound states. Up to now most PBE calculations have been based on SK_{pred} (docking) [18,34] where only the rigid binding reaction was modeled. Some experimental studies suggest [8,9] that conformational changes of both binding partners tRNA and aaRS upon the complexation reaction are small (mostly local arrangements occur upon binding) compared to other RNA-protein complexes [35].

By computing the electrostatic binding free energy of the various tRNA-aaRS complexes, over a specified range of salt concentration where the linearity between ΔG_{elec} and log[NaCl] holds we can determine the slope of this curve and compare it with experimental thermodynamic data (the slope of the linear plot of $\log K_{obs}$ versus log[NaCl], here termed SK_{obs}, where [NaCl] is the salt concentration) whenever it is available. Our slope of the curve ΔG_{elec} vs. log[NaCl] was obtained by a least-square fit of the calculated data, using an in-house script based on a Numerical Recipes algorithm [36]. The resulting slope is then our SK_{pred} which is related to SK_{obs} in Eq. (2.1).

2.6 Oligocationic binding model

According to the Record-Lohman model [10], which is based on the counterion condensation theory [11], the salt dependence of the binding constant can be interpreted from the following linear relationship assuming the absence of anion, hydration effects, conformational and/or protonation changes of both binding partners:

$$\frac{d\log K_{obs}}{d\log[NaCl]} = -Z\psi, \tag{2.3}$$

where Z represents the net charge of the oligocationic peptide (or number of cationic residues) or oligocationic protein patch (usually taken as the number of ion pairs, *i.e.*, ionic charge contacts between cationic side chains and phosphate groups near the binding interface) and ψ denotes the fraction of counter-ions (*e.g.*, Na^+) that is thermodynamically bound to the nucleic acid (fractional neutralization of phosphate charges by thermodynamic bound counterions). This simple linear relationship establishes a link between thermodynamics and structural information about the protein-nucleic acid complex [37].

The extension of the Record-Lohman oligocation binding model to larger proteins with both anionic and cationic residues is based on the assumption that the protein behaves locally as an oligocation and thus, SK_{obs} only reflects the interaction of the nucleic acid with locally cationic surface regions of the protein that interface with the nucleic acid. This implies that SK_{obs} only reflects the interaction of the nucleic acid with the charges at or near the binding interface, which seems at odds with the fact that electrostatic interactions are long-ranged and scale as the reciprocal of the distance ($1/r$).

Table 1: Calculated properties of Glutamyl and Glutaminyl tRNA-synthetase bound to their cognate tRNA.

PDB	#Residues		Charge(e)		#Charge-pairs[a]		SK[b]		
	Prot	RNA	Prot	Tot.	$r \leq 4$	$4 < r \leq 6$	LBP	NLPB	Exp. [8]
GluRS									
1G59	468	75	-2	-76	8/**4**	5/**4**	26.5	-2.2	-1.7±0.2
1N77	468	74	-2	-75	9/**2**	1/**7**	22.7	-2.5	-1.7±0.2
GlnRS									
1O0B	529	74	-12	-85	9/**0**	4/**3**	18.5	-3.1	-1.3±0.3
1QTQ	529	74	-12	-85	10/**0**	3/**3**	16.9	-3.4	-1.3±0.3

All calculations are based on the energy minimized aaRS-tRNA complexes. [a]Residues found within distance "r" Å from the amide nitrogen or carboxylate-oxygen atoms (bold numbers) to the nearest phosphate-oxygen atom in the RNA-chain. [b]$\mathrm{SK_{obs}} = d\log \mathrm{K_{obs}}/d\log[\mathrm{Na^+}]$. According to Eq. (2.1) in the text we assume that $\mathrm{SK_{pred}} = \mathrm{SK_{obs}}$ where $\mathrm{SK_{pred}} = -d\Delta \mathrm{G_{elec}}/d\log[\mathrm{Na^+}]$ is based on the linear and nonlinear Poisson-Boltzmann approach, here referred to as the LPB and NLPB, respectively. See text for more details.

3 Results and discussion

As shown in Figs. 1(a) and 1(b), respectively, the discriminative GluRS and GlnRS (from *E. coli.*) folds in different ways, such that the former is alpha-beta folded whereas the latter is mainly beta-folded. However, both GluRS and GlnRS are acidic. In fact, the GluRS and GlnRS with net charges of -2e and -12e, respectively, have a significant number of anionic residues distributed over the protein and some of these acidic residues are even located in the close vicinity of the tRNA (Fig. 2). In particular, GluRS has 4 anionic residues within 4 Å from the nearest phosphate group, whereas GlnRS has none (Table 1). But does the minimum distance really reflect pure charge-charge repulsions for anionic residues close to the phosphate-oxygens in the tRNA backbone? This question is partially answered by surveying of the hydrogen-bonding pattern between the aaRSs and their cognate tRNAs and by examining the electrostatic potential maps.

3.1 Hydrogen-bonding and electrostatic signature of GluRS bound to $\mathrm{tRNA^{Glu}}$

In Fig. 3, all charged protein-residues in the GluRS that have any of its atoms within 6 Å from any of the tRNA atoms are highlighted: red - acidic residues (Asp and Glu); blue - basic residues (Arg and Lys). Any of these residues that form hydrogen bond(s) to tRNA are colored darker and the remaining residues within 6 Å to the tRNA are in lighter colors. The tRNA is roughly shaped like the letter "L" since the tRNA loops into the anti-codon region (U33, C34, U35), which is the recognition site for the enzyme, and then back to the central crossing above a fairly neutral region without charged residues where it forms the corner portion of the "L". The vertical region of the "L" then passes

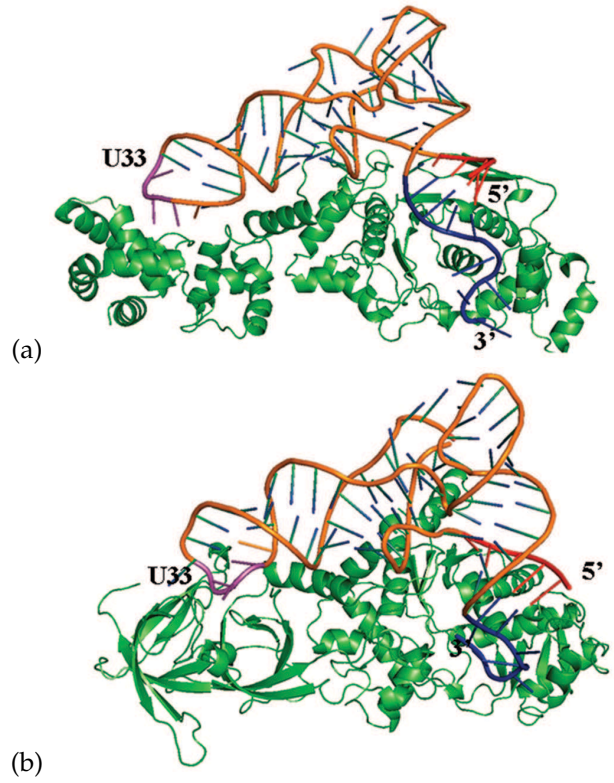

Figure 1: Schematic drawing of the tRNA synthetase in complex with its cognate tRNA. The RNA 5'-end is labeled and 3 RNA-residues are colored red. The anticodon stretch, bases 33-35 are colored in magenta with the first base, U33, labeled (residues 5'-YU^{33}C-3' for GluRS and residues 5'-YU^{33}G-3' for GlnRS). Five RNA-bases, preceding the 3' end are colored in blue, and the 3'-end is also labeled. (a) GluRS-tRNA^{Glu} (PDB id: 1G59). (b) GlnRS-tRNA^{Gln} (PDB id: 1QTQ). The pictures were generated with the PYMOL program. (http://pymol.sourceforge.net/).

through a highly charged region of both basic and acidic residues. All the basic residues in this region form hydrogen-bonds to tRNA.

It appears that four acidic residues form hydrogen bonds between the carboxylate group and the tRNA backbone hydrogen (Fig. 3). Interestingly, all these hydrogen bonds are formed with tRNA-residues near the terminal ends (C3 and C5 at the 5′-end and C73, A75 at the 3′-end, respectively). At the 5′-end, the absence of basic residues would make this part of the tRNA less tightly bound to the GluRS. There is also a significant number of positively charged residues that hydrogen-bonds to tRNA (Fig. 3), which favors tRNA-binding to the GluRS: The anti-codon region is anchored in a patch of positive residues that form hydrogen-bonds to the GluRS, and the central part of the tRNA-looping is rich in positive residues that are hydrogen-bonded to tRNA, and finally the 3′-end displays a solid anchor of positive residues (which surrounds two of the acidic residues that hydrogen-bonds to tRNA). However, a pattern of alternating positive/negative charged

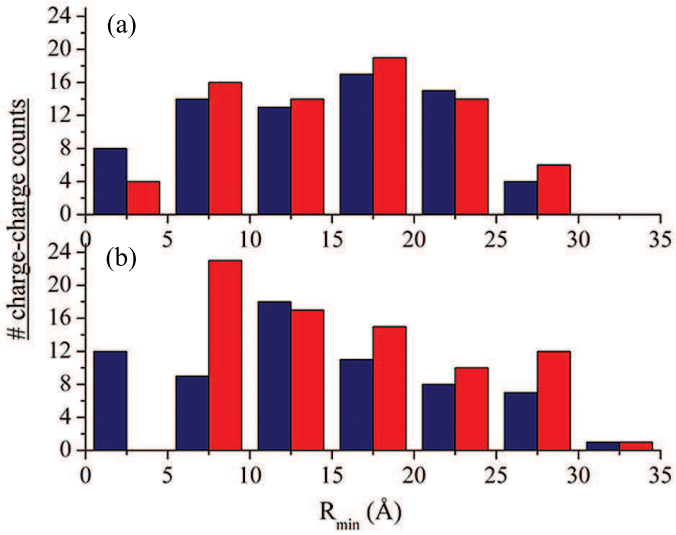

Figure 2: Shortest distance between $OD_{1,2}$, $OE_{1,2}$, $HN_{1,2}$ and NZ protein atoms and RNA $OP_{1,2}$ atoms: distribution of aaRS-tRNA charge-charge pairs for anionic (red) and cationic (blue) protein residues: (a) GluRS and (b) GlnRS. The structures were obtained from the RCSB Protein Data Bank with PDB ids: 1G59 and 1QTQ, respectively.

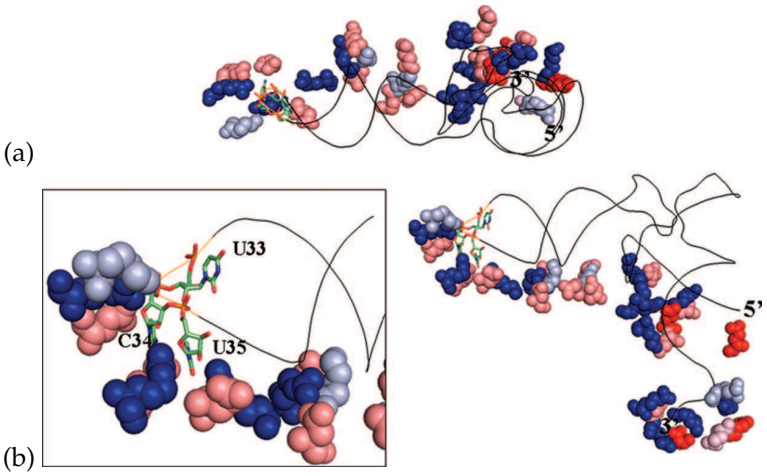

Figure 3: Distribution of GluRS charged amino-acids within 6 Å from any of the $tRNA^{Glu}$ atoms (shown as black ribbon). Negatively charged residues (Asp and Glu) are colored in red and positively charged residues (Arg and Lys) are colored in blue. Any residue that forms a hydrogen bond to tRNA is in darker color. Lighter color means that the residues do not form hydrogen bonds to tRNA, but is within 6 Å from the tRNA. The inset shows the anti-codon recognition site and the tRNA-bases are labeled from the 5'-end to the 3'-end. (a) View along the Z-plane and the vertical axis of the tRNA which forms an "L"-shape in binding to GluRS. (b) View along the X-Y plane. The pictures were generated with the PYMOL program. (http://pymol.sourceforge.net/).

residues that are within 6 Å from the tRNA-spine is observed. These residues do not form hydrogen-bonds (in lieu with the distance from the hydrogen to the acceptor atom is ≤ 2.4 Å), but indicate a balance of charges in the vicinity of tRNA.

This charge-balance is clearly seen in the electrostatic potential maps of the GluRS-$tRNA^{Glu}$ (Fig. 4) and we see that the two distinct "anchoring" sites - around the anti-codon binding region and the RNA-bases binding in the region of the 3′ end - generate a favorable potential for the tRNA. It is also clearly seen that these two main binding regions are separated by a less favorable binding region - around the crossing of the horizontal and vertical part of the "L", and that the environment around the 5′ - end is highly negative, and thus less favorable for tRNA-binding. It is interesting to note that the most positive potential regions in the maps (in green) correspond to the hydrogen-bonds that were captured by the minimization and analysis protocol.

Thus locally, it seems that the GluRS provide a high charge-density with areas of highly negative potentials in the RNA-binding interface, - if defined within 6 Å -, despite the fact that the overall net-charge of the enzyme is $-2e$.

3.2 Hydrogen-bonding and electrostatic signature of GlnRS bound to $tRNA^{Gln}$

Fig. 5 is organized in the same way as in Fig. 3, but depicts the GlnRS instead. We see that the 5′-end is surrounded by a number of positive residues forming direct hydrogen bonds to the tRNA. One acidic residue (Asp228) is found in this region and this residue forms two hydrogen bonds with the backbone of tRNA-bases G2 and G3. Unlike the GluRS (Fig. 3), however, the presence of basic residues would counterbalance the less favorable interaction from the acidic residues and thus make this part of the tRNA more tightly bound to the protein relative to the GluRS. The "L"-shape of the tRNA is apparent and the tRNA passes another acidic residue that hydrogen bonds to the backbone of G9 before it loops into the anticodon region (U33, G34, A35), which is the recognition site for the GlnRS. This region appears embedded in a very positive patch made up of basic residues that form hydrogen bonds to the tRNA. The tRNA then loops back and - in a similar manner to the GluRS - forms the corner of the "L" in a fairly neutral region, before the vertical portion of the "L" is highly stabilized by forming several hydrogen bonds to basic residues with the residues immediately preceding (A70, G71, C73, A74) the 5′-end of the tRNA. However, some basic and acidic residues are within the 6 Å, but without forming hydrogen-bonds to tRNA. This indicates - as for the GluRS - some sort of charge balance in the GlnRS (Fig. 5).

This charge-balance is reflected in the electrostatic potential maps of the GlnRS-$tRNA^{Gln}$ (Fig. 6) and we see that there are three main "anchoring" sites - near the 5′-end, around the anti-codon site and in the region of the 3′ end - that generate a favorable potential for the tRNA. It is also clearly seen that these three regions have a smaller portion of unfavorable binding region when compared to the GluRS (Fig. 4), but that there are areas of steeply negative potentials on the GlnRS surface. These areas are - however - located further away from the tRNA and beyond 6 Å. Again, we note that the most posi-

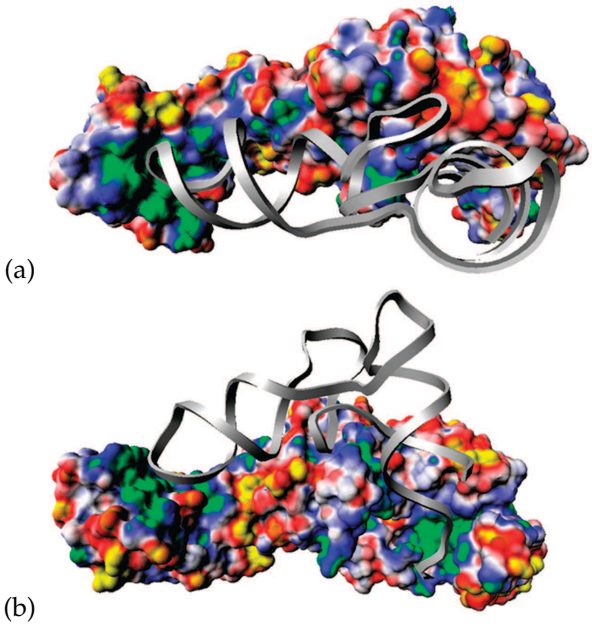

Figure 4: Electrostatic potential maps of the GluRS and a schematic ribbon representation of its cognate $tRNA^{Glu}$. The colors in both maps range from -2 kT/e to +2 kT/e from: Yellow-red (negative), white (neutral) and blue-green (positive). The maps are based on the minimized structure of PDB id:1G59: (a) oriented as in Fig. 3(a), and (b) oriented as in Fig. 3(b). The pictures were made with the VRML program. (http://www.nist.gov/).

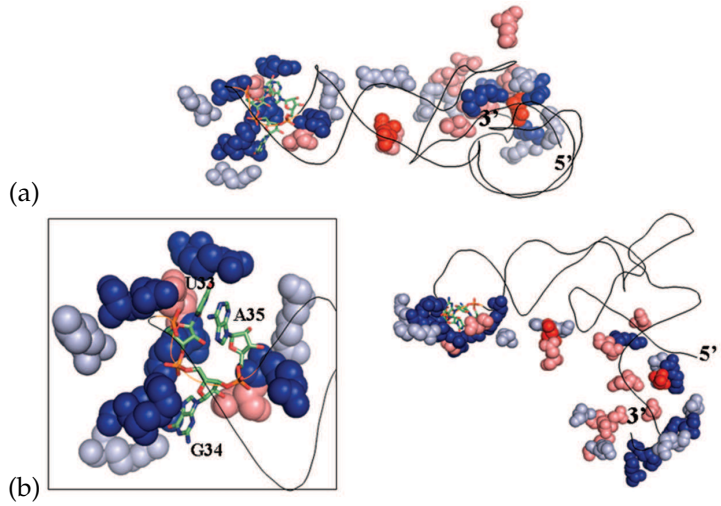

Figure 5: Distribution of GlnRS charged amino-acids within 6 Å from any of the $tRNA^{Gln}$ atoms (shown as black ribbon). Negatively charged residues (Asp and Glu) are colored in red and positively charged residues (Arg and Lys) are colored in blue. Any residue that forms a hydrogen bond to tRNA is in darker color. Lighter color means that the residues do not form hydrogen bonds to tRNA, but is within 6 Å from the tRNA. The inset shows the anti-codon recognition site and the tRNA-bases are labeled from the 5'-end to the 3'-end. (a) View along the Z-plane and the vertical axis of the tRNA which forms an "L"-shape in binding to GluRS. (b) View along the X-Y plane. The pictures were generated with the PYMOL program. (http://pymol.sourceforge.net/).

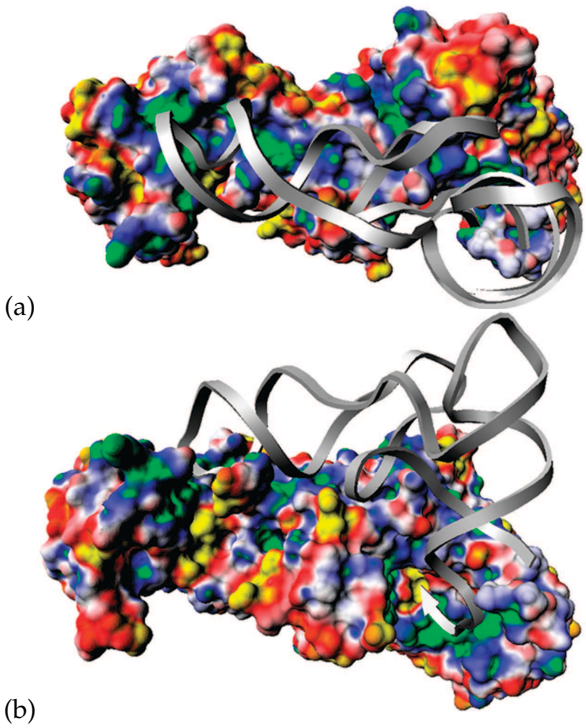

(a)

(b)

Figure 6: Electrostatic potential maps of the GlnRS and a schematic ribbon drawing of its cognate $tRNA^{Gln}$. The colors in both maps range from -2 kT/e to +2 kT/e from: yellow-red (negative), white (neutral) and blue-green (positive). The maps are based on the minimized structure of PDB id: 1QTQ: (a) oriented as in Fig. 5(a), and (b) oriented as in Fig. 5(b). The pictures were made with the VRML program (http://www.nist.gov/).

tive potential regions in the maps (in green) correspond to the hydrogen-bonds that were captured by the minimization and analysis protocol.

Thus locally, it seems that the GlnRS provide a more favorable environment for the tRNA-binding - if defined within 6 Å, - despite the fact that the overall net charge of this protein is -12e.

3.3 Salt dependence of the GluRS-$tRNA^{Glu}$ and GlnRS-$tRNA^{Gln}$ association process

Here we consider an intriguing association process where both binding partners: tRNA and aminoacyl-tRNA synthetase are negatively-charged [8, 38]. According to some experimental studies performed by different laboratories it has been found that the salt dependence of both noncognate and cognate ValRS, GluRS and GluRS binds to tRNA with the same mechanism [8, 38, 39].

From the slopes of the electrostatic binding free energy versus log[NaCl] linear plots obtained using our nonlinear PBE solver, SK_{pred} (from Eq. (2.1)) is -2.2 and -3.3, for the GluRS- and GlnRS-tRNA complexes, respectively. These results are in good agreement

with the experimental SK_{obs} values of -1.7 and -1.3 (Table 1). When taking into account the limitations in the computational protocol, a better agreement between SK_{pred} and SK_{obs} may involve properly modeling in the protonation-state of charged residues and conformational adaptability of binding partners. That is, assuming that electrostatics dominate in the salt dependence of the binding process.

When the linear PBE is employed on the GluRS and GlnRS in complex with their cognate tRNA, SK_{pred} is on average 24.6 and 17.7, respectively (Table 1). Here, the deviation of SK_{pred} from the experimental SK_{obs} values was considerably larger (by several orders of magnitude) and opposite in sign. This extremely pronounced salt dependence of the binding free energies is not in agreement with the experimental results [8]. We clearly demonstrate that the linear PBE can not be applied for examining the salt dependent behavior of these highly charged systems due to its reduced local screening effect.

3.4 SK_{obs} versus the oligocation binding model prediction

Some recent thermodynamic studies have shown that for the IHF-DNA and 1TF1-DNA complexes [14, 15] the oligocation binding model significantly overestimates the magnitude of SK_{obs}. Here, we examine if this is also the case for the tRNA-enzymes complexes.

Our analysis shows that the magnitude of the SK_{obs} values for both GluRS- and GlnRS-tRNA complexes are much lower than similar values obtained using the number of ionic contacts from our structural analysis (see Table 1) and applying the oligocation binding model (Eq. (2.3)). Based on this analysis we would predict a SK_{oligo} (not to be confused with that computed with the PBE, which we call SK_{pred}) value of ~ 11 considering that ~ 13 contacts are made between the phosphate backbone and the cationic enzymes residues that reside within 6 Å from the nearest phosphate group (see Table 1, data for 1G59 and 1QTQ). Another important aspect in this case is that variant lengths of the nucleic acid chain will produce different distance distributions in the number of charge-charge pairs. Therefore, assumptions about ion-pairs (or indeed any charge-pairs between protein-nucleic acid) based on structural information may not always be adequate.

3.5 Does a low SK_{obs} imply that the electrostatic contribution to binding is small?

We would like to point out that the rather small values of SK_{obs} do not imply that electrostatic interactions will have a small effect on the binding process. According to our results, the electrostatic contribution to binding for these aaRS-tRNA systems is much more unfavorable, mainly due the large less favorable Coulombic term for GlnRS-tRNA complexes and large and less favorable de-solvation term for the GluRS-tRNA complexes, when compared to the L11-RNA complex. In the latter RNA-protein complex the protein is cationic and has a significant number of cationic residues around the binding interface. Thus, one would expect that the magnitude of SK_{obs} should be large based on the oligo-

cation binding model. However, the absolute SK_{obs} values for L11-RNA complex [40] are low and comparable to the GlnRS-tRNA or GluRS-tRNA complexes, which have an even larger number of cationic protein-phosphate contacts spread over its larger binding interface. The electrostatic binding free energy for the L11-RNA binding reaction is significantly more favorable compared to aaRS-tRNA largely due to a favorable Coulombic term (in preparation). Thus, any conclusion about the significance of the electrostatic contribution to the binding free energy based on the values of SK_{obs} should not be made: A low SK_{obs} does not necessarily mean that the electrostatic contribution to the binding free energy is small.

3.6 Impact of protein charge-neutralization on SK_{pred}

To examine how the anionic protein residues affect SK_{pred} the following computer experiment was conducted: We "turned off" the Glu and Asp residues charges (*i.e.*, the charges on these residues were set to zero) at various distances as defined in the pair-wise minimum distance criteria (see Methods section). When the anionic residues are "turned off", a significant impact on the SK_{pred} values is observed (Fig. 7). It is interesting to note that the large number of anionic residues that are far from the binding interface also displays a significant impact on the SK_{pred}. Thus, it becomes clear that SK_{pred} is not solely determined by cationic or anionic residues near or close to the binding interface, or within 6 Å to the nearest phosphate group in the nucleic acid, but also by charged protein residues that are remote from the binding interface. This is in particular the case for anionic residues, whereas the cationic residues appear to have a similar impact within and above 6 Å.

From Fig. 7 one observes that the negatively charged enzyme residues have a much larger impact on SK_{pred} compared to the positively charged protein residues. Moreover, the anionic residues that are further than 6 Å have a larger impact relative to those closer than 6 Å probably due to the fact that there are a larger number of anionic residues farther in the GlnRS from the tRNA (See Fig. 2). This trend is more pronounced for the more negatively charged GlnRS enzymes when compared against the GluRS enzymes. On the other hand, it is interesting to note that the effect of "turning off" cationic residues both closer and further than 6 Å is similar. When the charges of anionic and cationic enzyme residues are modified (*i.e.* "turned off") a significant impact is seen in SK_{pred}. Together with Fig. 2, this implies that not only the distance of nearby interfacial charged residues influence the SK_{pred}, but also the remotely positioned charged residues are dictating the salt-mediated electrostatic behavior in protein-nucleic acid binding (Fig. 7). The difference in "turning off" cationic residues for the two GluRS-tRNA structures (pdb code: 1G59 and 1N77) is due to the different number of cationic residues within 6 Å as also can be seen in Table 1. In the same way, the similarity for the corresponding GlnRS-tRNA structures when "turning off" the cationic residues are reflected by the same number of cationic residues within 6 Å to the nearest phosphate-group.

Hence, interactions that stems from anionic enzyme residues even distant to the in-

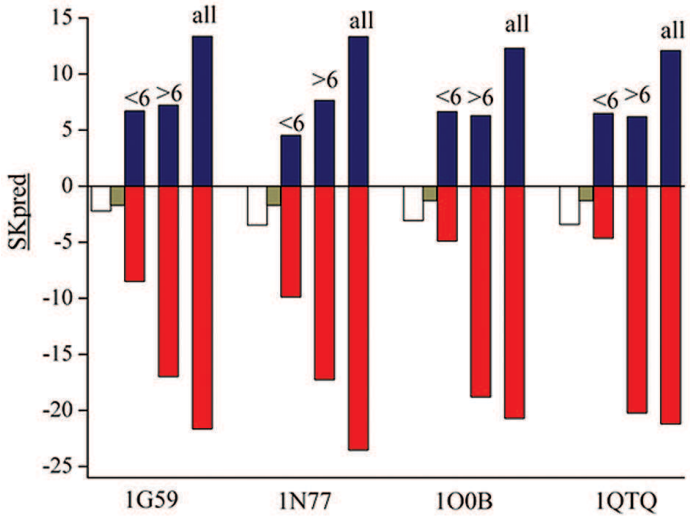

Figure 7: Effects on SK_{pred} by "turning off" charged residues: (i) at distances "r" from the tRNA for enzyme residues with "r" less than 6 Å (ii) protein residues further away than 6 Å; (iii) or all protein residues turned off. Only the non-linear PBE was used in this computer experiment. Red bars depict the effect of neutralizing anionic residues and blue bars the corresponding effect for neutralizing cationic residues. The SK_{pred} for the full potential (open bar) is shown together with the experimental SK_{obs} (green bar). The PDB ids are indicated on the x-axis: GluRS: 1G59 and 1N77; GlnRS: 1O0B and 1QTQ.

terface with tRNA contribute significantly to the total salt effect. These results reinforce the importance of accounting for the long-range nature of non-specific electrostatic interactions.

4 Conclusions

Even if the linear and nonlinear PBE predict similar electrostatic binding free energies [28], it is clear from our studies that the predicted salt-dependent electrostatic behavior can be very different. Based on our results here and a previous study together with ongoing research in our lab, we conclude that the linear solution to the PBE should not be used to model salt-mediated electrostatic effects for charged ligand-nucleic acid association processes. We showed that the SK_{pred} from the nonlinear solution to the PBE is in good agreement with the experimental SK_{obs}, and correctly captures the salt-mediated electrostatic interactions.

Long-range electrostatic behavior for proteins/peptides bound to nucleic acids is reflected in the SK_{obs}, but cannot always be explained with the elegant oligocationic formulation (Eq. (2.3)). This model was successfully designed for predictions in the binding of oligocationic chains - such as oligoarginines/lysines - to nucleic acids, and does remarkably well in these kinds of systems [10]. However, one cannot use this simple relationship to compare the number or count the number of ionic interactions in protein-nucleic acid

complexes when acidic residues glutamate and aspartate are incorporated in the protein matrix. Our results indicate that anionic protein residues both near and far from the binding interface or any nucleic acid, have a significant effect on SK_{pred}. In fact, the anionic residues that are farther from the tRNA have an even larger effect compared to those closer in and have a much larger impact on SK_{pred} compared to the cationic residues. Thus, for the tRNA-enzyme complexes considered here, the cationic residues appear to be less influential compared to the anionic protein residues in controlling SK_{obs}, although the effect is still significant (Fig. 7). Thus, there is no simple correlation between SK_{obs} and structural or energetic information of ion-pairs in these cases. Direct contacts based on the so-called charge-charge pairs defined as the minimum distance between amide nitrogen or carboxylate oxygen atoms to the nearest phosphate-oxygen on the RNA/DNA spine, may also obscure actual hydrogen bonds that are formed between the amino-acid side-chain and the RNA. This does not rule out that the charge-charge repulsion affects the salt-dependence in protein/peptide nucleic-acid association, but depicts compensations in unfavorable interactions by stabilizing hydrogen-bond formations. Therefore, one should be cautious in defining boundaries or thresholds for delimiting the number of charge-charge contacts based on a specific distance.

Future theoretical and experimental studies will be essential in order to unravel the physical origin for the magnitudes of the SK_{obs}. The underlying mechanism is likely to be complex and dominated by electrostatic interactions, but probably also involves other effects not accounted for by the mean-field based nonlinear PBE approach.

Acknowledgments

This work is supported by NSF-CHEM-0137961 (to MOF) and in part by the Institute for Mathematics and its Applications with funds provided by the National Science Foundation.

References

[1] P. S. Ray, A. Arif and P. L. Fox, Macromolecular complexes as depots for releasable regulatory proteins, Trends Biochem. Sci., 32 (2007), 158-164.
[2] A. M. Stock, V. L. Robinson and P. N. Goudreau, Two-component signal transduction, Annu. Rev. Biochem., 69 (2000), 183-215.
[3] S. W. Lee, Y. S. Kang and S. Kim, Multifunctional proteins in tumorigenesis: Aminoacyl-tRNA synthetases and translational components, Curr. Proteomics, 3, (2006), 233-247.
[4] D. Tworowski, A. V. Feldman and M. G. Safro, Electrostatic potential of aminoacyl-tRNA synthetase navigates tRNA on its pathway to the binding site, J. Mol. Biol., 350 (2005), 866-882.
[5] D. Thompson, P. Plateau and T. Simonson, Free-energy simulations and experiments reveal long-range electrostatic interactions and substrate-assisted specificity in an aminoacyl-tRNA synthetase, Chem. Bio. Chem., 7 (2006), 337-344.

[6] D. Thompson and T. Simonson, Molecular dynamics simulations show that bound Mg+2 contributes to amino acid and aminoacyl adenylate binding specificity in aspartyl-tRNA synthetase through long range electrostatic interactions, J. Biol. Chem., 281 (2006), 23792-23803.
[7] D. F. Green and B. Tidor, Escherichia coli glutaminyl-tRNA synthetase is electrostatically optimized for binding of its cognate substrates, J. Mol. Biol., 343 (2004), 435-452.
[8] R. Banerjee, A. K. Mandal, R. Saha, S. Guha, S. Samaddar, A. Bhattacharyya and S. Roy, Solvation change and ion release during aminoacylation by aminoacyl-tRNA synthetases, Nucleic Acids Res. 31 (2003), 6035-6042.
[9] S. Sekine, O. Nureki, A. Shimada, D. G. Vassylyev and S. Yokoyama, Structural basis for anticodon recognition by discriminating glutamyl-tRNA synthetase, Nat. Struct. Mol. Biol., 8 (2001), 203-206.
[10] M. T. J. Record, T. M. Lohman and P. deHaseth, Ion effects on ligand-nucleic acid interactions, J. Mol. Biol., 107 (1976), 145-158.
[11] G. Manning, The moleculat theory of polyelectrolyte solutions with applications to the electrostatic properties of nucleotides, Qrtly. Rev. Biophys., 11 (1978), 179-246.
[12] R. M. Saecker and M. T. Record, Protein surface salt bridges and paths for DNA wrapping, Curr. Opin. Struct. Biol., 12 (2002), 311-319.
[13] S. Bergqvist, M. A. Williams, R. O'Brien and J. E. Ladbury, Reversal of halophilicity in a protein-DNA interaction by limited mutation strategy, Structure, 10 (2002), 629-637.
[14] A. Grove, Surface salt bridges modulate DNA wrapping by the type II DNA-binding protein TF1, Biochemistry, 42 (2003), 8739-8747.
[15] J. A. Holbrook, O. V. Tsodikov, R. M. Saecker and M. T. Record, Jr., Specific and non-specific interactions of integration host factor with DNA: Thermodynamic evidence for disruption of multiple IHF surface salt-bridges coupled to DNA binding, J. Mol. Biol., 310 (2001), 379-401.
[16] H. Kim, E. Jeong, S-W. Lee and K. Han, Computational analysis of hydrogen bonds in protein-RNA complexes for interaction patterns, FEBS Lett., 552 (2003), 231-239.
[17] S. Jones, D. T. A. Daley, N. M. Luscombe, H. M. Berman and J. M. Thornton, Protein-RNA interactions: A structural analysis, Nucl. Acids Res., 29 (2001), 943-954.
[18] C. García-García and D. Draper, Electrostatic interactions in a peptide RNA complex, J. Mol. Biol., 331 (2003), 75-88.
[19] S. Sekine, O. Nureki, D. Y. Dubois, S. Bernier, R. Chenevert, J. Lapointe, D. G. Vassylyev and S. Yokoyama, ATP binding by glutamyl-tRNA synthetase is switched to the productive mode by tRNA binding, EMBO J., 22 (2003), 676-688.
[20] T. L. Bullock, N. Uter, T. Amar Nissan and J. J. Perona, Amino acid discrimination by a class I aminoacyl-tRNA synthetase specified by negative determinants, J. Mol. Biol., 328 (2003), 395-408.
[21] V. L. Rath, L. F. Silvian, B. Beijer, B. S. Sproat and T. A. Steitz, How glutaminyl-tRNA synthetase selects glutamine, Structure, 6 (1998), 439-449.
[22] B. R. Brooks, R. E. Bruccoleri, B. D. Olafson, D. J. States, S. Swaminathan and M. Karplus, CHARMM: A program for macromolecular energy, minimization, and dynamics calculations, J. Comp. Chem., 4 (1983), 187-217.
[23] A. D. MacKerell, Jr., D. Bashford, M. Bellott, R. L. Dunbrack, Jr., J. D. Evanseck, M. J. Field, S. Fischer, J. Gao, H. Guo, S. Ha, D. Joseph-McCarthy, L. Kuchnir, K. Kuczera, F. T. K. Lau, C. Mattos, S. Michnick, T. Ngo, D. T. Nguyen, B. Prodhom, W. E. Reiher, III, B. Roux, M. Schlenkrich, J. C. Smith, R. Stote, J. Straub, M. Watanabe, J. Wiórkiewicz-Kuczera, D. Yin and M. Karplus, All-atom empirical potential for molecular modeling and dynamics studies

of proteins, J. Phys. Chem. B., 102 (1998), 3586-3616.
[24] N. Foloppe and A. D. MacKerell. Jr., All-atom empirical force field for nucleic acids: I. Parameter optimization based on small molecule and condensed phase macromolecular target data, J. Comp. Chem., 21 (2000), 86-104.
[25] A. Brünger and M. Karplus, Polar hydrogen positions in proteins: Empirical energy placement and neutron diffraction comparison, Proteins, 4 (1988), 148-156.
[26] P. J. Steinbach and B. R. Brooks, New spherical-cutoff methods for long-range forces in macromolecular simulation, J. Comp. Chem., 15 (1994), 667-683.
[27] D. J. Barlow and J. M. Thornton, Ion-pairs in proteins, J. Mol. Biol., 168 (1983), 867-885.
[28] A. H. Boschitsch and M. O. Fenley, Hybrid boundary element and finite difference method for solving the nonlinear Poisson-Boltzmann equation, J. Comp. Chem., 25 (2004), 935-955.
[29] K. Sharp, Salt dependence, entropic and enthalpic contributions to free energy in the nonlinear Poisson-Boltzmann model, Biopolymers, 36 (1995), 27-243.
[30] M. K. Gilson and B. H. Honig, Calculation of electrostatic potentials in an enzyme active site, Nature, 330 (1987), 84-86.
[31] A. H. Boschitsch and M. O. Fenley, A new outer boundary formulation and energy corrections for the nonlinear Poisson-Boltzmann equation, J. Comp. Chem., 28 (2007), 909-921.
[32] R. V. Polozov, M. Montrel, V. V. Ivanov, Y. Melnikov and V. S. Sizozhelezov, Transfer RNAs: Electrostatic patterns and an early stage of recognition by synthetases and elongation factor EF-TU, Biochemistry, 45 (2006), 4481-4490.
[33] A. Lagunavicius, S. Grazulis, E. Balciunaite, D. Vainius and V. Siksnys, DNA binding specificity of MunI restriction endonuclease is controlled by pH and calcium ions: Involvement of active site carboxylate residues, Biochemistry, 36 (1997), 11093-11099.
[34] M. Zacharias, B. Luty, B. Davis and J. McCammon, Poisson-Boltzmann analysis of the lambda repressor-operator interaction, Biophys. J., 63 (1992), 1280-1285.
[35] N. Leulliot and G. Varani, Current topics in RNA-protein recognition: Control of specificity and biological function through induced fit and conformational capture, Biochemistry, 40 (2001), 7947-7956.
[36] W. H. Press, S. A. Teukolsky, W. T. Vetterling and B. P. Flannery, Numerical Recipes: The Art Of Scientific Computing, Cambridge University Press, 2007.
[37] P. H. von Hippel, From "simple" DNA-protein interactions to the macromolecular machines of gene expression, Annu. Rev. Biophys. Biomol. Struct., 36 (2007), 7-105.
[38] J-P. Ebel and J. Bonnet, Influence of various factors on the recognition specificity of tRNAs by yeast valyl-tRNA synthetase, Eur. J. Biochem., 58 (1975), 193-201.
[39] G. Krauss, D. Riesner and G. Maass, Mechanism of discrimination between cognate and noncognate tRNAs by phenylalanyl-tRNA synthetase from yeast, Eur. J. Biochem., 68 (1976), 81-93.
[40] D. GuhaThakurta and D. E. Draper, Contributions of basic residues to ribosomal protein L11 recognition of RNA, J. Mol. Biol., 295 (2000), 569-580.